

Seasonal variations of the near surface layer parameters over the Antarctic ice sheet in Princess Elizabeth Land, East Antarctica

Chen Zhigang(谌志刚)¹, Bian Lingen(卞林根)¹, Xiao Cunde(效存德)¹, Lu Longhua(陆龙骅)¹ and Ian Allison²

¹ Chinese Academy of Meteorological Sciences, Beijing 100081, China

² Australian Arctic Division and Antarctic CRC, Hobart, Tasmania, 7001, Australia

Received July 24, 2007

Abstract Analysis of sensible heat flux (Q_h), latent heat flux (Q_e), Richardson number (Ri), bulk transport coefficient (C_d) and katabatic winds are presented by using the meteorological data in the near surface layer from an automatic weather station (AWS) in Princess Elizabeth Land, East Antarctica ice sheet and the data of corresponding period at Zhongshan station in 2002. It shows that annual mean air temperature at LGB69 is -25.6°C , which is 16.4°C lower than that at Zhongshan, where the elevation is lower and located on the coast. The temperature lapse rate is about $1.0^\circ\text{C}/110\text{m}$ for the initial from coast to inland. The turbulence heat flux at LGB69 displays obvious seasonal variations with the average sensible heat flux $-17.9\text{W}/\text{m}^2$ and latent heat flux $-0.9\text{W}/\text{m}^2$. The intensity ($Q_h + Q_e$) of cooling source is $-18.8\text{W}/\text{m}^2$ meaning the snow surface layer obtains heat from atmosphere. The near surface atmosphere is near-neutral stratified with bulk transport coefficients (C_d) around 2.8×10^{-3} , and it is near constant when the wind speed higher than 8m/s . The speed and the frequency of easterly Katabatic winds at LGB69 were higher than that at Zhongshan Station.

Key words eastern Antarctic ice sheet; turbulent flux; katabatic wind; seasonal variation

1 Introduction

95% of the Antarctic land is permanently snow-covered, which is adjacent to the southern ocean, and acting as an important channel connecting southern oceans (i.e., the south Pacific, Atlantic and Indian Oceans). As a result, interactions between ice and air and between sea and air over the Antarctica exert significant impacts on extra-tropical atmospheric circulations as well as on East Asian climate^[1, 2, 3]. In view of the severity of Antarctic climate most of perennial weather stations are on the coasts and only several make observations inland (e.g., South pole station and Vostok station). Therefore, compared to data from coastal stations, only paucity is provided from inland stations, thus making more difficult the analysis of interactions between inland ice sheet and atmosphere. Automatic weather station (AWS) network has been working in Antarctica since the 1980s. It in-

cludes one set up by US in Rose ice shelf^[4], the one by Australian scientists to the south of Casey station^[5] and the one established in the ice sheet around Mizuho station by Japanese meteorologists^[6]. It forms a basis for the research of the turbulent flux exchange between ice sheet and air inland. Ian *et al* (1993)^[7] made analysis of 100~140°E climate characteristics by means of AWS data, resulting a close relationship of surface temperature, pressure and wind to the ice sheet condition. Cheng *et al* (1999)^[8] investigated the weather/climate features of the Grove Mountains of the continent. An AWS named as LGB69 over Princess Elizabeth land was founded in 2002 under the cooperation between Chinese Antarctic Administration and Australian Antarctic Division. Based on AWS data throughout 2002, in order to better understand the differences in the features of near-surface layer meteorological parameters between coastal and inland Antarctica, which plays a crucial role of concerning interaction among ice sheet and atmosphere and prediction katabatic wind around Zhongshan station, the present paper attempts to investigate the annual variations in turbulent fluxes and other elements, and to compare with those simultaneously collected at Zhongshan station.

2 Materials and methods

2.1 Site and Meteorological Measurements

LGB69 is located at 70°06'S, 77°04'E and 1850 m above ms.l, 160 km from the east coast (see Fig. 1) and setup in January, 2002 on Princess Elizabeth land by the 17th Chinese Antarctic expedition. The AWS was developed and calibrated at Australian Antarctic Division before transport to the Antarctic. It is consisted of a 4 m height tower, measuring gradient wind and temperature at 1 m, 2 m and 3 m high above surface, as for relative

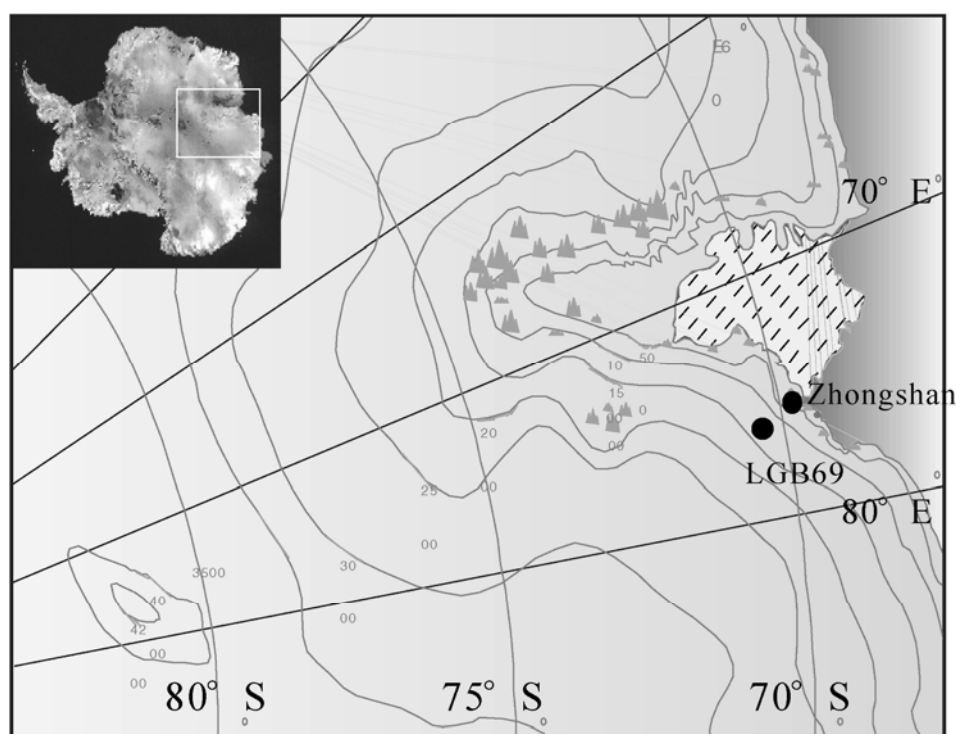


Fig. 1 Geographical position of LGB69 and Zhongshan Station

humidity, wind direction and solar radiation at a 4 m height, for snow temperature at 0.1 m, 1 m, 3 m and 10 m depths, and for pressure and snow cover with their models and resolution presented in Table 1. Sampling frequency is once an hour and the data transmit on real-time to the global telecommunication system (GTS) via the ARGOS satellite. The data can be downloaded from ARGOS website through FTP or from GTS directly.

Table 1 The models and sensor resolutions of sensors at LGB69 AWS

Sensors	Types	Sensor resolution
Air temperature	FS23D thermistor (individually calibrated)	0.02°C
Relative humidity	Vaisala HM P45D	3%
Wind speed	AAD cup anemometer	0.2 m/s
Wind direction	Aanderra 3590 vane	6°
Snow height	Campbell SR50-45	Scientific 1 cm
Solar radiation	Middleton EP08 Paroscientific	0.1 MJ m ⁻²
Pressure	Digiquartz 6051A FS23D thermistor	0.1 hPa
Snow temperature	(individually calibrated)	0.02°C

In close proximity to the ice sheet, Zhongshan station is situated at 69°22'S, 76°22'E on Larsson Hills inside Prydz Bay and snow-covered all the year round except December-March during which much of snow is melted around the station. Katabatic winds prevail in the summer half year (October-March) and LGB69 is upstream of Zhongshan station so that AWS data serve as an important source for studying the occurrence and development of these winds at Zhongshan station.

2.2 Flux Profile Methods

The data of 3-level winds and temperatures as well as the flux profile relationship are applied to compute turbulent fluxes and the associated characteristic parameters over the ice sheet. Before calculating sensible heat (H) and latent heat (LE) fluxes, the Monin-Obukhov similarity theory is used to compute frictional velocity (u^*), temperature scale (T^*), characteristic specific humidity (q^*) and Monin-Obukhov length. The expressions shown in the following:

$$u_* = k(u_j - u_i) / \left[\ln \left| \frac{\zeta_j}{\zeta_i} \right| - \Psi_{sm}(\zeta_j) + \Psi_{sm}(\zeta_i) \right] \quad (1)$$

$$\theta_* = \theta_j - \theta_i / \left[\ln \left| \frac{\zeta_j}{\zeta_i} \right| - \Psi_{sm}(\zeta_j) + \Psi_{sh}(\zeta_i) \right] \quad (2)$$

$$q_* = q_j - q_i / \left[\ln \left| \frac{\zeta_j}{\zeta_i} \right| - \Psi_{sh}(\zeta_j) + \Psi_{sh}(\zeta_i) \right] \quad (3)$$

$$L = - u_*^3 / \rho C_p (\theta_i + \theta_j) / 2kgQ_h \quad (4)$$

And the result as

$$Ri = \frac{2g \sqrt{Z_i Z_j} \ln(\zeta_j / \zeta_i) (\theta_j - \theta_i)}{(\theta_j + \theta_i) (u_j - u_i)^2} \quad (5)$$

$$Q_h = - \rho_p u_* \theta \quad (6)$$

$$Q_e = - \rho_v u_* q \quad (7)$$

$$C_d = 4u_*^2 / (u_i + u_j)^2 \quad (8)$$

It is noted that through (1) to (5), k ($= 0.4$) denotes Von Karman constant, u the wind velocity, q the specific humidity obtained from $q = 0.622 \times \frac{e}{p}$, where e the vapor pressure with respect to ice is computed from ice temperature and saturated humidity, θ the potential temperature acquired from $\theta = T(P/P_0)^{0.286}$, L the Obukhov length, Ri the Richardson number as the stability parameter, g the gravitational acceleration. $\Psi_{sh}(\zeta_i)$ and $\Psi_{sn}(\zeta_i)$ are the universal functions of (ζ_i) , or as the functions of correcting stratification that denote the deviation of wind speed, temperature and specific humidity from the related logarithmic profiles under neutral stratification. ζ_i is a dimensionless height in the form as (9)

$$\zeta_i = (Z_i - Z_0) / L \quad (9)$$

in which Z_i stands for observing height and Z_0 for the surface roughness that is obtained via fitting of wind speeds at different levels. ζ_i has its expression similar to that for ζ . It is noted that forms of universal function are roughly analogous to each other when using different observations except for some difference in calculated parameters. The universal function by Dyer *et al.* (1970)^[9] is adopted, which defined as

When

$$\xi < 0$$

$$X_i = (1 - 16\xi)^{1/4}$$

$$\Psi_{sn}(\xi) = 2 \ln[(1 + X_i)/2] - \ln[(1 + X_i^2)/2] - \tan^{-1}(X_i) + \pi/2 \quad (10)$$

$$\Psi_{sh}(\xi) = 2 \ln[(1 + X_i^2)/2] \quad (11)$$

when

$$1 > \xi > 0$$

$$\Psi_{sn}(\xi) = \Psi_{sh}(\xi) = -5\xi \quad (12)$$

when

$$\xi > 1$$

$$\Psi_{sn}(\xi) = \Psi_{sh}(\xi) = -5 \ln(\xi) \quad (13)$$

All of them are nonlinear equations that are solved with iteration method. In such a way that initial values of U_{*0} and L_0 are found under presumed neutral stratification before getting universal functions through inserting these initial values into (10) to (13), which are then substituted into (1) to (8) for iteration. Generally, the iteration is convergent and reaches < 1% relative errors in results after 4~5 iteration.

3 Results

3.1 Annual variations of meteorological element

As we know, variations of meteorological elements are under great impacts of elevation and geographic position of the station. To compare observations from LGB69 to those from Zhongshan station, the pressure are reduced to sea level values by means of their monthly

mean temperatures, with monthly mean pressure, temperature, specific humidity and wind velocity in 2002. Fig. 2 displays their variations on an annual basis. From the yearly curves of pressure, the trends are much the same except for the difference of ~ 10 hPa in the average between them for two stations, with the maxima and minima observed in the same months, and the pressures are considerably higher in the winter than in the summer half.

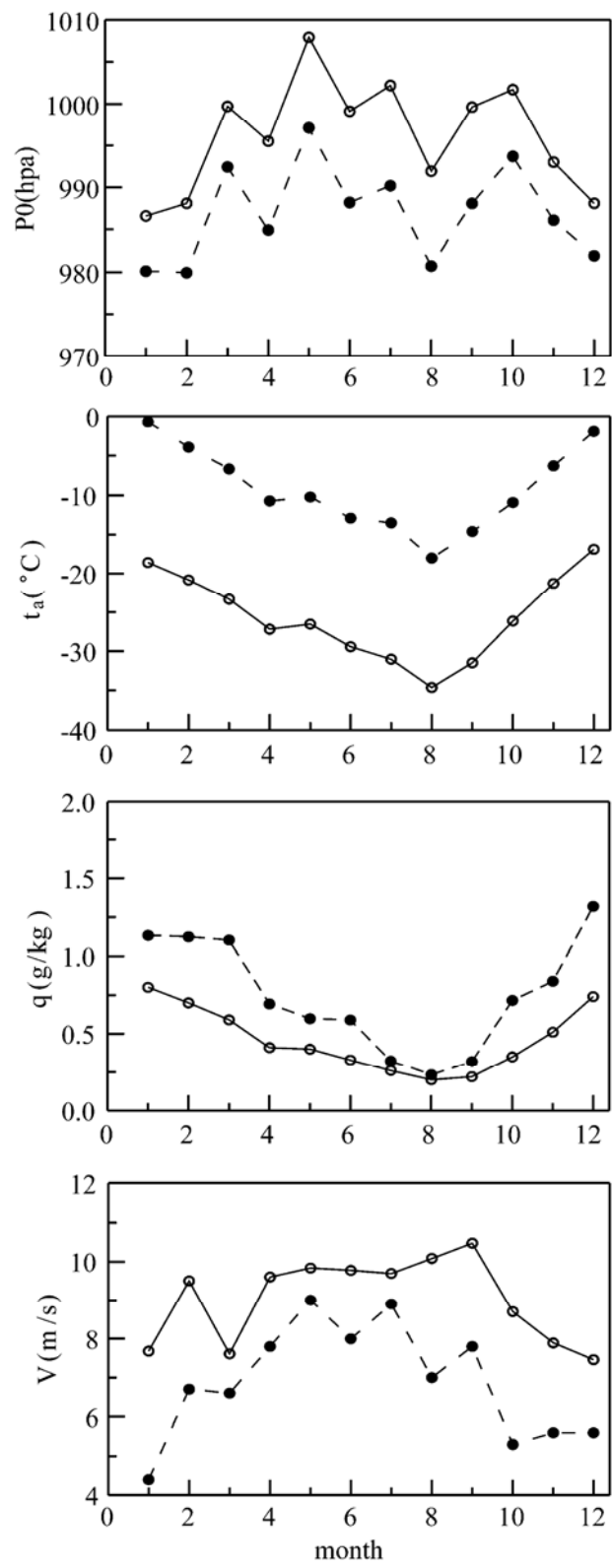


Fig. 2 Annual variations of air pressure (P_0), air temperature (t_a), humidity (q) and wind speed (V) at LGB69 (solid line) and at Zhongshan (dashed line).

year (April–September versus October–March), with the correlation coefficient of 0.95

(Fig 3), indicative of the fact that both stations are under the same influence of a large-scale synoptic system. As for yearly mean temperature, it is -25.6°C at LGB69, about 16.4°C lower compared to that at Zhongshan station, meaning that the temperature drops roughly 1°C for 110 m rise in height at a 10 km interval inland. For LGB69 the coldest (hottest) temperature is often below -40°C (-10°C) in winter (summer), a yearly variation that which is similar, on the whole, to that at Zhongshan station, with temperature changing fast in the summer and slowly in winter half year, indicating the core-free feature of wintertime temperature variation (Fig 2). This is approximately true for other Antarctic weather stations.

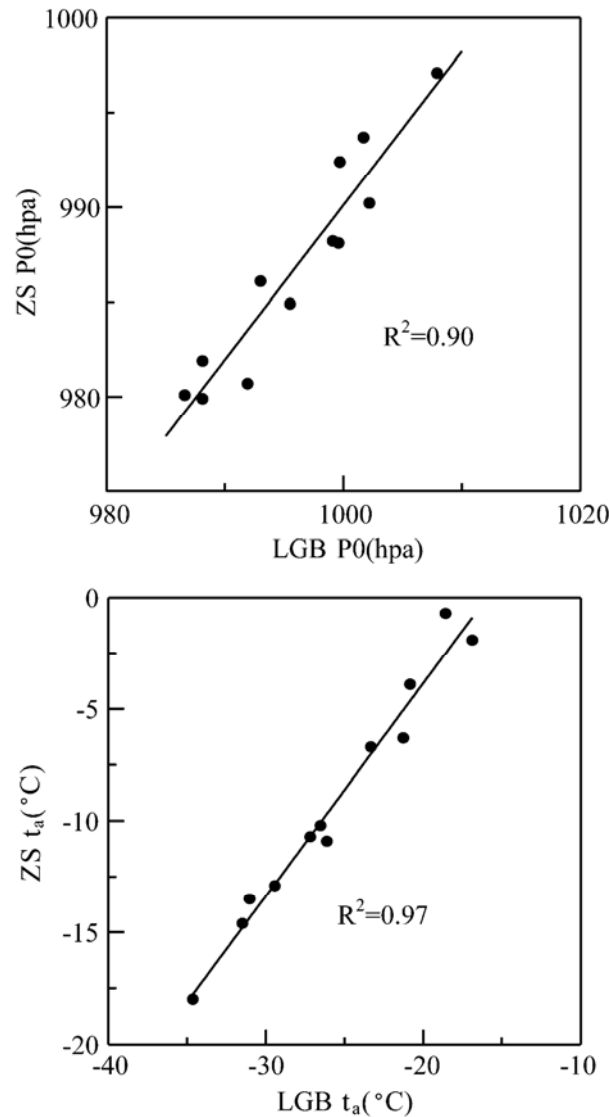


Fig 3 Relations of monthly mean air pressures (P_0) and temperatures (t_a) between LGB69 and Zhongshan in 2002

Monthly mean humidity is lower at LGB69 than at Zhongshan station, the data from both showing an apparent annual variation, with the higher happening in December and January, and the lower in August. The difference in mean humidity between the stations in the summer is significant, indicating that the lowered humidity is due to the fact that LGB69 is located inland at higher elevation with colder temperature in contrast to considerably higher humidity at Zhongshan station that is on the coast and exposed to relatively high temperature, with plentiful vapor coming into the air. In the winter half year, on the other

hand, much of the sea is frozen nearby Zhongshan station, thus greatly reducing preventing vapor into the air, so that the difference becomes very small in humidity between the two sites.

Annual mean wind is smaller at LGB69 compared to M izuho station at the same latitude (9.0 m/s vs 11 m/s)^[6], with its monthly maxima in excess of 10 m/s in September. As evidenced in Fig. 2, monthly mean winds are all higher at LGB69 than those at Zhongshan station. The differences in winds between the stations are markedly greater in the summer than in the winter half year because of katabatic winds prevalent at LGB69 during the summer.

Fig. 4 shows the yearly variation of temperature in the snow depth of 0.1 , 1 , 3 , 0 and 10 m at LGB69. It is obvious that the temperature in at 0.1 m depth snow is influenced by thermal conductivity from the surface, resulting in very distinct annual variation, with monthly mean minimal and maximal temperature of -35.2° in September and -18.3°C in January, respectively. The annual temperature amplitudes of snow are 16.9°C and 12.7°C , 4.8°C and 0.6°C for at the snow depths of 0.1 , 1 , 3 , 0 and 10 m respectively, which indicates that the annual amplitude of snow temperature decreases with increasing snow depth. Maximal and minimal temperature in depth snow of 3 , 0 and 10 m occur lagging behind 0.1 and 1 , 0 m . They were in January and September at 0.1 and 1 , 0 m respectively, and in March and October for 3 , 0 m , as well as in August and February for 10 , 0 m . This evident illustrates that there is little effect of thermal condition below 1 , 0 m on the near surface snow temperature. In other words, the thermal exchange of snow and air appears mainly above 1 , 0 m .

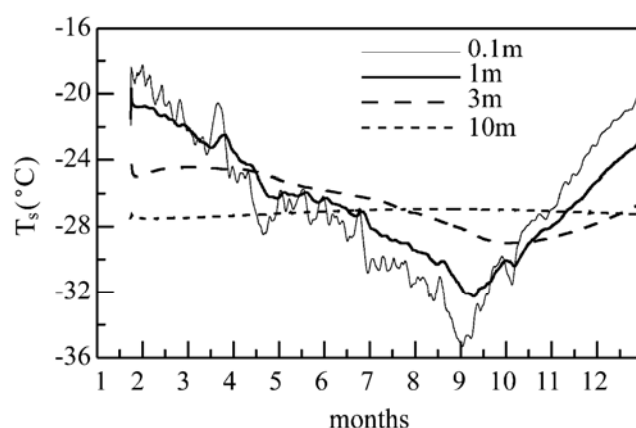


Fig. 4 Annual variations of snow temperature (TS) in different deepness

3.2 Turbulent fluxes

Fig. 5 presents annual variation of turbulent fluxes for at LGB69 calculated by means of 3-level gradient data and the similarity theory. It is indicated that the annual variation of sensible heat flux is quite remarkable. The monthly mean values are negative except in December. From October to March heat is very small with -5.4 W/m^2 and from April to September it reached -32.3 W/m^2 . Its annual average is -17.9 W/m^2 , and means that the snow surface gains heat from the atmosphere. The annual average of latent heat is as low as -0.9 W/m^2 with smaller annual variation as the inland area is less influence by marine with the extremely low temperature and very small amount of latent heat released from sublimation.

mation of snow or ice as well throughout a year. However the annual variation of latent heat flux is much smaller compared to that of the sensible heat.

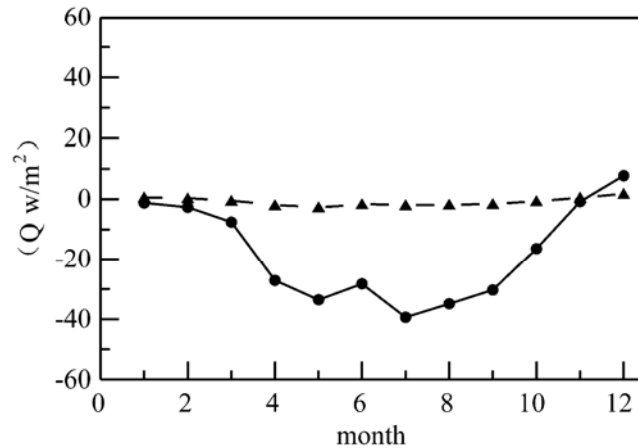


Fig. 5 Annual variations of sensible heat flux (Q_h) (solid line) and latent heat flux (Q_e) (dashed line) at LGB69.

From the equation of surface energy balance ($Q_h + Q_e$ [GW/6]) the intensity of heat source can be defined as $Q_h + Q_e > 0$ referred to as a thermal source and $Q_h + Q_e < 0$ the opposite as a cold source. Following this definition, the LGB69 annual mean flux of $Q_h + Q_e$ is -18.8 W/m^2 , e.g. the surface layer can be as a cold source and obtained from the atmosphere. The minimum monthly mean of $Q_h + Q_e$ is -41.5 W/m^2 in July and the maximum is 9.4 W/m^2 in December. In the summer (winter) half year $Q_h + Q_e$ is -5.3 W/m^2 (-34.3 W/m^2), indicating that surface layer acts as a weak (strong) cold source with heating by air in year round.

In Fig. 6 the mean diurnal variation of heat flux is shown as an average for the summer and winter seasons. In the day time (06:00–18:00) the heat flux is higher than zero, with peak value of 41.4 W/m^2 . It is negative in the nocturnal time. The daily amplitude reaches 69.1 W/m^2 . There is almost no significant daily variation with constant about -35 W/m^2 in the winter. This can be interpreted as heating the surface layer with longer sunshine duration and stronger solar radiation for the daytime leading to the transfer of sensible heat into air while radiation cooling the surface layer in the nighttime and the heat from air is transferred downward to the surface. Especially in the period of polar day, the surface layer is heated by air.

As the temperature of the surface is below 0°C there is small amounts of latent heat by heat of sublimation absorbed and condensation released of the snow surface. In summer the daily maximum of latent heat value is 7.5 W/m^2 with daily range of 11 W/m^2 . On the other hand, in the winter daily the heat is almost no variation with small fluctuating of -1.8 W/m^2 . Therefore latent heat plays a negligible role on the interaction between snow and air in the Antarctic inland.

3.3 Bulk transfer coefficient and atmospheric stability

Atmospheric stability is one of the importance parameters on the study of boundary layer. In term of definition of the criteria (Ri) developed by Richardson in determination of

the atmospheric stability, $R < 0$ denotes instability, $R = 0$ neutral stability, $R > 0$ stability.

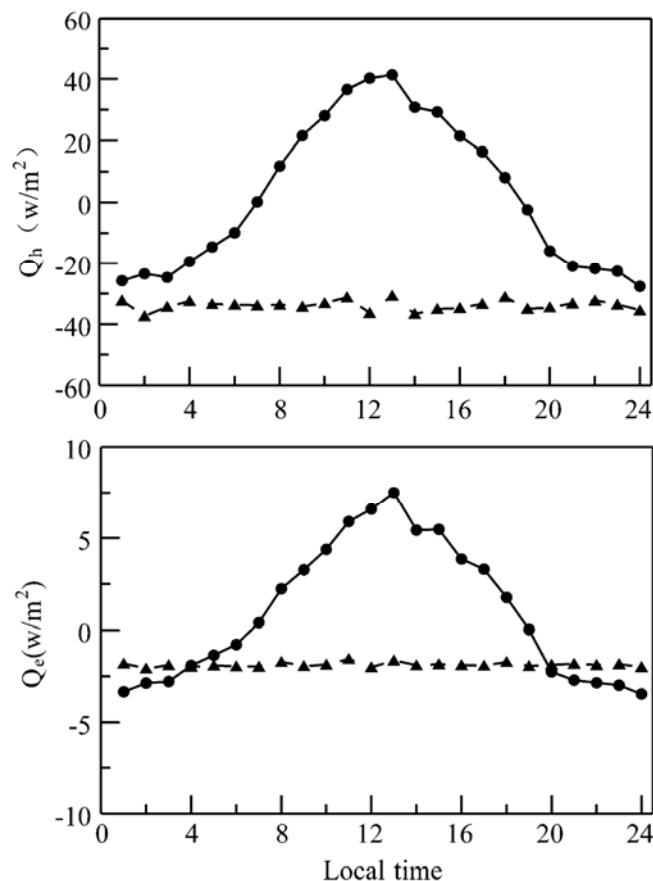


Fig 6 Diurnal variations of sensible heat flux (Q_h) (solid line) and latent heat flux (Q_e) (dashed line) in summer and winter at LGB69

In practice, $-0.025 < R < 0.025$ refers to a neutral or near-neutral stratification. In the whole year 4696 valid samples for R_i (Richardson number) at 2.5 m level are obtained. There are 4208 samples for neutral or near-neutral stratification, 368 and 120 samples for steady and unsteady stratification, respectively. They are 89.6%, 7.8%, and 2.6% of the valid samples respectively. It is deduced that the atmosphere of the surface layer dominates neutral or near-neutral stratification and less convective weather throughout the year in the Antarctic inland.

The bulk transport coefficient is an important factor for dynamic and thermal research of the boundary layer. The coefficient of momentum flux (C_d) represents the drag of turbulent friction, depending largely on dynamical effect of wind speed. Fig 7 gives their correlation. It can be seen that the coefficient is larger with smaller wind speed and it approaches a steady value with wind speed in excess of 8 m/s. The linear relation between C_d and wind speed (u) at 2 m height is obtained as the form of $C_d = 3.8 \times 10^{-6} \times \log(u) + 2.6045 \times 10^{-3}$.

The relationship between the coefficient and stratification is close. The coefficients of different stratification is determined to be 2.6×10^{-3} for the near-neutral, 1.8×10^{-3} for the steady and 3.9×10^{-3} for the unsteady stratification, respectively, obtained by fitting the annual data. However, our coefficients in this paper are larger compared to those reported by Qu *et al.* (1989) for the Japanese Antarctic Mizuho station. The possible reason is

associated with difference in snow surface conditions and katabatic wind effect between the two regions

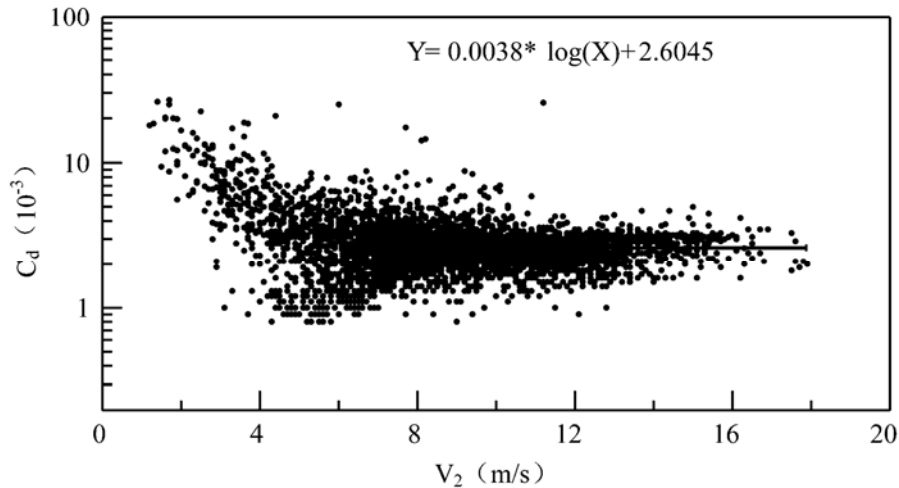


Fig 7 Relations between wind speed (V_2) at 2m and Bulk transport coefficient of momentum (C_d) at LGB69

4 Katabatic winds

Zhongshan station is located at the fringe of the Antarctic ice sheet where katabatic winds is a mainly weather system, which is caused by the mutual impact from the topographic of the eastern Antarctic plateau and a high pressure system over the continent^[10]. Fig 8 shows the diurnal variation of monthly mean wind speed for the summer and winter at LGB69 and Zhongshan station. The variation is apparent with the daily maximum of 10.0 m/s occurred on 11:00LT. and daily minimum of 6.5 m/s on 20:00LT. in summer at

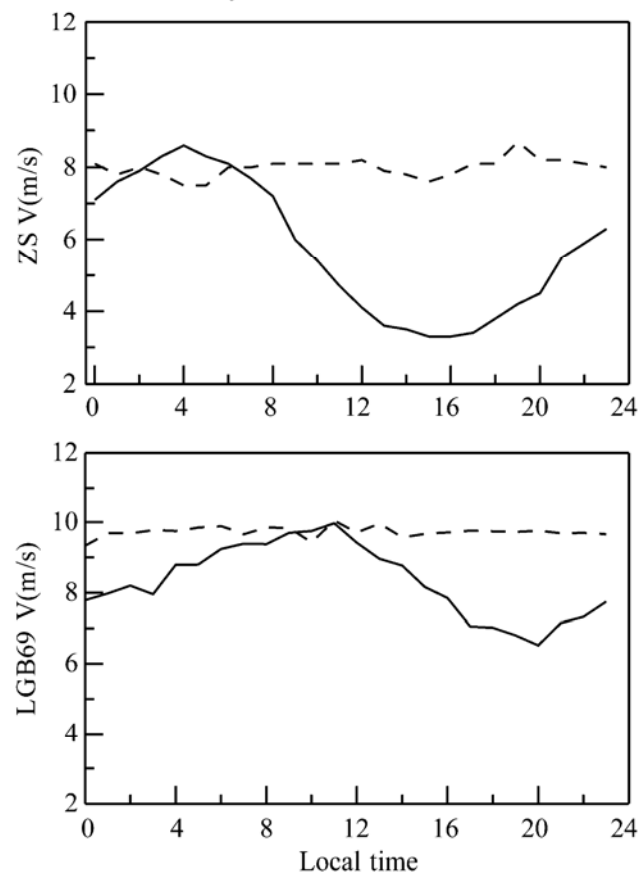


Fig 8 Diurnal variation of wind speed in summer (solid line) and winter (dashed line) at Zhongshan (ZS) and LGB69

LGB69. It is indicated that the LGB69 region prevails katabatic winds in the summer and which not appear in the winter. The pattern of the diurnal wind speed at LGB69 corresponds to the katabatic displayed in other Antarctic regions. This is because the strength of radiation cooling on the snow surface layer is relative larger and leads to the wind speed the nighttime and while the strength of radiation cooling in the daytime becomes weaker and while the wind speed decreases in summer. From Fig. 6 it can be seen that there is no diurnal variation of the wind at both stations in the winter that means the solar radiation forcing is too negligible to cause the katabatic winds.

Fig. 9 presents the frequencies of wind directions at 8 orientations in 2002 for LGB69 and Zhongshan station. It can be seen that for LGB69 the frequencies of NEN, NEE and SEE orientations are higher and the NEE is most prevalent. The region of LGB69 is one of the significant Antarctic katabatic area.

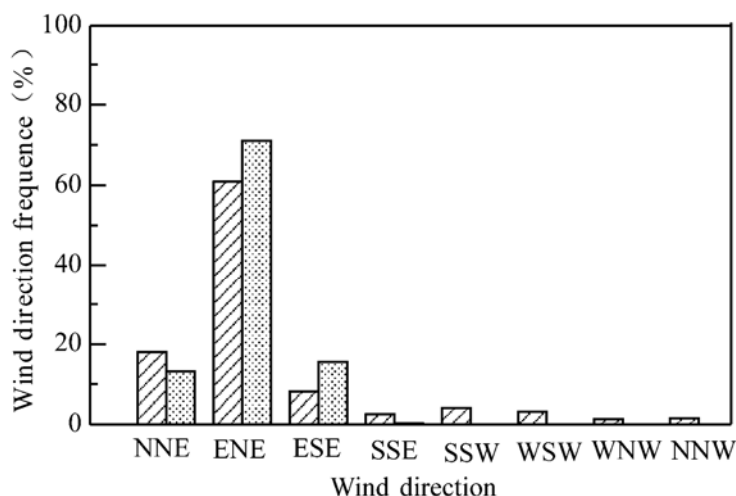


Fig. 9 Frequency of eight orientations of wind direction appeared at Zhongshan (slash) and LGB69 (dot).

For Zhongshan station located at the downstream region of LGB69 and where the wind speed exhibits apparent diurnal variation with the daily peak of 8.6 m/s at 04:00 LT. and daily minimum of 3.3 m/s at 16:00 LT. in summer. The summer winds at Zhongshan station are smaller compared with that at LGB69 and the consistence time of the katabatic wind is shorter. Also frequency of prevailing wind direction is almost the same, too. Meanwhile the winds in the winter is no distinct diurnal variation. However the region of Zhongshan station is under the great effect of katabatic winds coming upstream in LGB69 area region and the previous deduction also given by Bian *et al.*^[11].

5 Conclusion and discussion

Based upon the comparison of meteorological elements from LGB69 and Zhongshan station and on the analysis of calculated turbulent parameters for LGB69, the following conclusions can be discussed.

(1) As LGB69 located at the Antarctic inland of the higher elevation and snow-covered all the year round, its annual mean temperature is -25.6°C , with about 16.4°C lower than that at Zhongshan station. It means that temperature drops by $1.0^{\circ}\text{C}/110\text{m}$ rise in elevation at a 10 km interval inland. The characteristic of annual variation of temperature

for both stations are basically similar, the temperature changes fast in the summer half year (Oct – Mar) and slowly in the winter half year (Apr – Sep). The change shows a “core-free” winter.

(2) There is apparent annual variation of sensible heat (Q_h) and the annual mean flux is -17.9 W/m^2 , that atmosphere is heating the snow surface. The yearly variation of latent heat (Q_e) is greatly smaller than that in sensible heat and its yearly average is -0.9 W/m^2 . The annual average of $Q_h + Q_e$ is -18.8 W/m^2 , with sharing of -5.3 W/m^2 for summer half year and -34.3 W/m^2 for winter half year. It is indicated that the strength of heat transferred from air to surface is over 6 times as high in the winter as in the summer half year.

There is a distinct diurnal variation of sensible heat flux with daily amplitude of 69.1 W/m^2 in summer. The latent heat flux is significantly higher in summer than that in winter with the daily amplitude of 11 W/m^2 . Winter diurnal variations of sensible and latent heat are not obvious.

(3) Based on analysis of Ri obtained in 2002 for atmospheric stability, near-neutral stratification is dominant in the surface layer at LGB69 and less convective weather happening. Correspondingly the coefficient of bulk transport (C_d) is 2.6×10^{-3} in the near-neutral case, 1.8×10^{-3} for the steady and 3.9×10^{-3} for the unsteady stratification. The amplitude of C_d depends on wind velocity. It approaches a constant value at when $> 8 \text{ m/s}$. The linear relation between C_d and wind speed (u) is obtained as the form $C_d = 3.8 \times 10^{-6} \times \log(u) + 2.6045 \times 10^{-3}$.

(4) The annual mean wind speed is 9.0 m/s at LGB69, with maximum monthly mean over 10.0 m/s occurred in September where easterlies prevails all the year round as a source of typical katabatic winds. As Zhongshan station located in downstream region of LGB69, despite wind speed where is smaller than that at LGB69 the frequencies of easterly winds is basically same as at LGB69 indicating the katabatic at Zhongshan station is affected greatly by sinking flows resulted from radiation cooling of the inland ice sheet upstream.

Acknowledgements This work was supported by NSF of China (No. 40575033) and MOST of China project (No. 200603805005). The authors thank Xia Limin, Xu Xiaoxing, Yan Ming, Gao Xincheng and Wang Fudong for very helpful during installation of the AWS in the 18th Chinese Antarctic expedition. The authors also wish to thank Dr Gao Zhiqiu for his comments.

References

- [1] Chen JN, Zhang Y (1998): Characteristics of Antarctic sea ice extent and its relations to SST in the tropical Pacific ocean. *transaction* 20(3): 134–139.
- [2] Xie SM, Bao CL (1996): Interaction between bipolar cold air and tropical heat air. *Acta Oceanologica Sinica* 18(2): 41–49.
- [3] Zhen QY, Wang YH (1999): Simulation of sea ice abnormal in Weddell Sea of Antarctica impacts on atmospheric circulation and weather of Northeast Asia in earlier summer. *Acta Oceanologica Sinica* 21(2): 40–48.
- [4] Stearns CR, Savage M (1986): Automatic weather station 1980–1981 Antarctic. *JUS* 14(5): 46–59.

- [5] Ian A, Morrissy JV (1983): Automatic weather stations in the Antarctic Aust Meteorol Mag 31: 71– 76
- [6] Qu SH, Shan NG (1989): Observational turbulent flux of momentum and sensible heat Antarctic Research 1(4): 1– 11.
- [7] Ian A, Gerd W, Uwe R (1993): Climatology of the East Antarctic ice sheet (100°E– 140°E) Derived from automatic weather stations J Geophys Res 98 (D5).
- [8] Chen YJ, Lu LH, Bian LG (1999): Weather characteristics in summer over G rover Mountain area in East Antarctic Chinese Journal of Polar Research 11(4): 291– 300
- [9] Dyer AJ, Hick BB (1970): Flux-gradient relationships in the constant flux layer Quart J Roy Meteorol soc 96 715– 721.
- [10] Hu SL (1993): The observation and study report on marine meteorology of Chinese Seventh Antarctic Research Expedition wintering at Zhonshan station Ocean Forecast 10(2): 51– 57.
- [11] Bian LG, Xue ZF, Lu CG (1998): Characteristics of climate in short term over Larssman hill Antarctic Research 10(1): 38– 46